Experimental Study on Fatigue Characteristics for Aluminium and Al-SiC Composite Material Edge Crack Specimens under Flexural Loading Conditions

Shanmugavel P. [#1], Bhaskar G.B. [#2], Chandrasekaran M. [#3]

[#1] Research Scholar, Anna University, Chennai, 600025, Tamilnadu, India
Department of Aeronautical Engineering, Kalaignar Karunanidhi Institute of Technology, Coimbatore, Tamilnadu, 641402, India
[#2] Department of Mechanical Engineering, Tagore Engineering College, Chennai, Tamilnadu, 600048, India
[#3] Department of Mechanical Engineering, Vels University, Chennai, Tamilnadu, 600117, India.
[1] pshanmugavel66@gmail.com
[2] bhaskarang01@yahoo.com
[3] chandrasekar2007@gmail.com

***Abstract*—Crack propagation studies on an Aluminium plate and Aluminium-Silicon Carbide composite plate under three point bend test conditions were done experimentally and the results so obtained been compared between Isotropic Aluminium and Aluminium-Silicon Carbide composite materials. The specimens with different crack length (a) to the depth (d) ratios (a/d Ratios) were prepared and the fracture characteristics of the specimens with different a/d ratios have been obtained experimentally and analyzed. The analysis has been done for both the Isotropic Aluminium and Aluminium-Silicon Carbide composite material specimens with different a/d ratios. A comparative analysis between the fracture characteristics of the Aluminium and Aluminium-Silicon Carbide composite material specimens for the same a/d ratio has been done and the results been plotted. Also the fractography at the cracked surface of the Aluminium and Aluminium-Silicon Carbide composite material specimens were undertaken along with the microstructures of these specimens. An attempt has been made to relate the fracture location and propagation to the microstructure of the material specimens.**

Keyword-Crack Propagation, Aluminium, Aluminium-Silicon Carbide Composite, fracture characteristics, microstructures

I. INTRODUCTION

Low-cost, light weight aluminium matrix composites have a good potential for application to aerospace structures [1]. Aluminium is a very light metal with a specific weight of 2.7 g/cm^3, about a third that of steel. The use of aluminium in vehicles reduces dead-weight and energy consumption while increasing load capacity. Its strength can be adapted to the application required by modifying the composition of its alloys. Aluminium naturally generates a protective oxide coating and is highly corrosion resistant. Different types of surface treatment such as anodizing, painting or lacquering can further improve this property. It can be melted, cast, formed and machined much like these metals and it conducts electric current. In fact often the same equipment and fabrication methods are used as for steel.

Aluminium-Silicon Carbide, AlSiC, pronounced ‘alsick’ is a metal matrix composite consisting of aluminium matrix with silicon carbide particles. It has high thermal conductivity (180–200 W/m K), and its thermal expansion can be adjusted to match other materials, e.g. silicon and gallium arsenide chips and various ceramics. AlSiC composites are suitable replacements for copper-molybdenum (CuMo) and copper-tungsten (CuW) alloys. They can be used as heat sinks, substrates for power electronics (e.g. IGBTs and high-power LEDs), heat spreaders, housings for electronics, and lids for chips, e.g. microprocessors and ASICs. The aluminium matrix contains high amount of dislocations, responsible for the strength of the material.

Advances in material synthesis technologies have spurred the development of a new class of materials, called Functionally Graded Materials (FGMs), with promising applications in aerospace, transportation, energy, electronics and bio-medical engineering. An FGM comprises a multi-phase material with volume fractions of the constituents varying gradually in a pre-determined and designed profile, thus yielding a non-uniform microstructure in the material with continuously graded properties. In applications involving severe thermal gradients, eg., thermal protection systems, FGMs exploit the heat, oxidation and corrosion resistance of

ceramics and the strength, ductility and toughness of metals [2]. Marin [3] list out the fields of applications of the FGMs as thermal barrier coatings for space applications, nuclear fast breeder reactors etc. Review articles available on FGMs include articles on research and development [4], property modelling [5], [6], manufacturing [7], [8], fracture mechanics [9], [10] and crack propagation [11]. Damage tolerance and defect assessments for structural integrity of FGM components require knowledge of the fracture behaviours of FGMs. For ceramic/metal FGMs, cracks generally nucleate near the ceramic surface exposed to the environment and grow towards the metal side. When a crack extends into the metal rich region, the substantial plastic deformation in the background FGM invalidates simple crack growth models based on linear-elastic crack tip analysis.

A. Experimental and Finite Element Models for Fracture Analysis

Finite element methods have been extensively used by majority of the researchers especially in the case of functionally graded materials. The arbitrary variations in material properties in chosen directions make the finite element modelling an effective tool to deal with. Linear analysis is performed in case of Linear Elastic Fracture Mechanics (LEFM). Only brittle materials, like diamond remain elastic even at the crack tip where stresses are high. Even in case of brittle materials most of them have some anelastic deformation close to the crack tip. The presence of plastic zone near crack tip in case of ductile materials necessitates the use of Elastic-Plastic Fracture Mechanics (EPFM). Tilbrook et. al. [12] used the finite element analysis to study the fracture behaviour of FGMs under flexural loading conditions. Li et. al. [13] have used the multiple isoparametric finite element method to obtain the mode I SIFs for FGM solid cylinders and found that the material property distribution affects the stress intensity factors to a great extent. The behaviours of embedded crack and external crack are different. Zhang and Paulino [14] investigated the dynamics of mixed mode fracture using cohesive zone modelling. It is found that the cohesive zone approach is effective in fracture evolution characteristics in homogenous and graded materials. Kim [15] has developed a finite element method for analysis of orthotropic FGMs with arbitrarily oriented cracks. The stress-intensity factors for mode I and mixed mode are evaluated. Comparison is made using modified crack closure techniques. Comi and Mariani [16] used an extended finite element model to study the propagation of cracks, and checked with the simulation of four points bending tests on notched beams. The energy release rates and propagation angles are calculated by varying the elastic properties as continuous gradients. Tilbrook et. al. [17] used finite element method to estimate crack-tip stress fields and propagation paths and compared with experimental results. Three dimensional finite element models have been used for the analysis of three dimensional cracks. Shim et. al. [18] used three dimensional finite element models to study the effect of material gradation on SIFs and K-dominance.

Jin et al [19] proposed a cohesive zone model to study the elastic-plastic crack growth in FGMs, which is an extended TTO model and analysed the titanium-beta-titanium single-edge notch bend specimen. Walters et al [20] used the FEM solutions and J-integral values to obtain the set of stress intensity factors for varied crack sizes and aspect ratios in FGMs under mode I loading conditions. Afsar et. al. [21] studied the problem of required material distribution to have the required fracture characteristic for an FGM cylinder. Afsar and Anisuzzaman [22] used a generalized method to obtain stress intensity factor of a thick-walled FGM cylinder. Hvizdos et al [23] experimentally studied the mechanical properties using indentation methods. Shock resistance using indentation quench method for an alumina/Zirconia FGM referred with the published literature.

B. Micro-structural Studies

Wang [24] has studied the micro-structural effects on the tensile and fracture behaviour of aluminium casing alloys A356/357and concludes that the transition from trans-granular to inter-granular fracture mode happens with the increase in the ductility of the alloys. Mcdanels [1] has analysed the stress-strain, fracture and ductility behaviour of aluminium matrix composites containing discontinuous silicon carbide reinforcement and implies on the suitability of the low-cost, light weight aluminium matrix composites for application to aerospace structures. Devi et. al. [25] have dealt on the micro-structural aspects of aluminium silicon carbide metal matrix composite and concludes that the silicon carbide inter metallic particles in the grain boundaries can influence the fracture behaviour. Micromechanics based models are used to predict the fracture behaviour of functionally graded composites. Li et. al. [26] discusses how the functionally graded WC-Co cemented carbide exhibit the toughness variations based on the microstructure and found that the structure character and so the stresses distribution state is a critical factor for fracture toughness. Lambers et. al. [27] have used the digital image correction (DIC) measurements and microscopy to study the influence of stresses due to bainitic phase transformations on the crack growth behaviour. Lee et. al. [28] used the finite element method based micromechanical analysis to study the fracture behaviour of functionally graded foams. Cannillo et. al. [29] used microstructure based computational models for crack propagation in glass-alumina FGMs and also compared the results with experimental results.

C. Present Study

The present paper deals with the experimental studies on isotropic aluminium and aluminium-silicon carbide composites to determine the maximum and peak load carrying capacities given with different initial crack length

to depth ratios. The fractography at the cracked surface of the specimens are done and also the microstructures of these specimens. An attempt has been made to relate the fracture location and propagation to the microstructure of the material specimens.

II. Materials and Experimental Methods

The materials chosen for experimental studies include isotropic aluminium, and Aluminium-Silicon Carbide (Al-SiC) composite materials. The test methods include the three point bend test to evaluate the fracture characteristics of the specimens. Also the fracture location, propagation microscopes and the microstructures of the specimens were studied using metallurgical microscopes.

A. Test Methods

The three point bending flexural test provides values for the modulus of elasticity in bending, flexural stress, flexural strain and the flexural stress-strain response of the material. The main advantage of a three point flexural test is the ease of the specimen preparation and testing. However, this method has also some disadvantages: the results of the testing method are sensitive to specimen and loading geometry and strain rate. Figure 1 shows the schematic of the three point bend test and the fixture used for three point bend test is shown in Fig. 2.

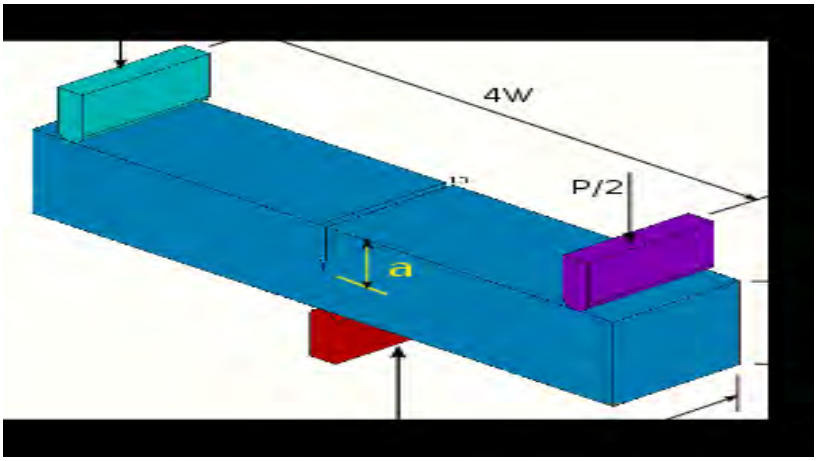

Fig. 1. Schematic of Three Point Bend Test

B. Test Specimens

The test specimens were prepared to the size of 152 mm x 38 mm x 6 mm as required by the fixture of the machine. For the aluminium bar, since the material has to be fabricated accurately, the material was cast with additional allowances of 2 mm on all sides.

The casting was machined to obtain the required dimensions of 152 mm x 38 mm x 6 mm. An edge crack in the form of wire cut was introduced for the different a/d ratios of 0.1, 0.2, 0.3, 0.4 and 0.5 on different specimens, where ‘a’ is the initial crack length and ‘d’ is the depth of the specimen. Thus the depths of edge crack introduced on different specimens for depth of 6 mm are 0.6 mm, 1.2 mm, 1.8 mm, 2.4 mm and 3 mm for the a/d ratios chosen. Two sets of 5 specimens were prepared for each of the aluminium and aluminium-silicon carbide composite materials.

The three point bend test was done using the universal tensile test rig. A fatigue load at the feed rate of 0.1mm/min was applied on the specimens to obtain the fatigue characteristics. The Al-SiC composite specimen was prepared in the same manner as that of aluminium except for the casting process, in which, while casting the 25 percent by weight of silicon carbide powder is added to the molten aluminium and stirred. The stirring is done in parallel with the addition of silicon carbide. The dimensional aspects of the test specimens and methods adopted are the same for both the aluminium and aluminium-silicon carbide composite materials.

The fixture used for three point test is shown in Fig. 2. This fixture is used on an universal tensile test rig. The testing equipment has the capability to load at the specified rate precisely and also capture the load versus displacement data at fine intervals. The data are stored into the computer automatically, and the reports are generated in the form of plots and also tabulated values.

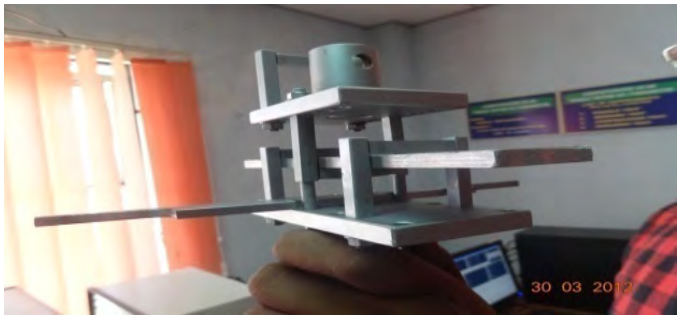

Fig. 2. Fixture for Three Point Bend Test

Figure 3 shows the test specimens used for three point bend test. The specimens are pre-cracked as per the required a/d ratio. As the load is applied at a fixed rate of 0.1 mm/min., the crack which is kept opposite to loading point opens up and slowly propagates along the depth direction till the final fracture occurs.

Fig. 3. An Aluminium Specimen with crack and Multiple Al-SiC Specimens with cracks in the depth direction

At this point, the specimen could no longer take load. The fixture is released from the testing equipment and the specimen is taken up for further studies under microscope.

III. Experimental Results and Discussions

The experimental test results for the isotropic aluminium and aluminium-silicon carbide composite materials are given. The plots depict the load versus deformation curve for the applied load in the form of feed rate of 0.1 mm/min. The plot gives the results in the form of break load carrying capacity, peak load carrying capacity, maximum displacement, displacement at break load, stress and stiffness values for the test specimens with different a/d ratios. The results obtained from the experimental studies on the aluminium specimens in the form of break load carrying capacity, peak load carrying capacity, maximum displacement, displacement at break load, stress and stiffness values for the test specimens with different a/d ratios are given in Table I.

TABLE I
Experimental Results for Aluminium Specimens

Parameter	**a/d Ratio**				
	0.1	**0.2**	**0.3**	**0.4**	**0.5**
Peak Load, N	1932	1706.4	1206.3	912.1	725.7
Break load, N	1762	362.9	245.2	186.3	147.1
Peak Displacement, mm	0.41	1.02	0.8	0.72	0.67
Break Displacement, mm	0.44	1.06	1.03	1.23	1.26
Proof Stress, N/mm^2	6.2	6.3	3.9	3.3	3.7
Stiffness, N/mm	1.2	1.1	1.4	1.9	2.1
ENG UTS, N/mm^2	10.1	8.9	6.3	4.8	3.8
True UTS, N/mm^2	10.1	9	6.4	4.8	3.8

The results obtained from the experimental studies on the aluminium-silicon carbide specimens in the form of break load carrying capacity, peak load carrying capacity, maximum displacement, displacement at break load, stress and stiffness values for the test specimens with different a/d ratios are given in Table II.

TABLE III
Experimental Results for Aluminium-Silicon Carbide Specimens

Parameter	a/d Ratio				
	0.1	**0.2**	**0.3**	**0.4**	**0.5**
Peak Load, N	2118.3	1667.2	1353.4	1078.8	784.6
Break load, N	2010	343	274.6	225.6	156.9
Peak Displacement, mm	0.53	1.15	0.94	0.78	0.94
Break Displacement, mm	0.55	1.27	1.09	1.15	1.25
Proof Stress, N/mm^2	5.6	6.6	6.2	4.7	3.7
Stiffness, N/mm	1.3	1.2	1.4	1.7	1.4
ENG UTS, N/mm^2	11	8.7	7	5.6	4.1
True UTS, N/mm^2	11.1	8.8	7.1	5.7	4.1

The results obtained for both the isotropic aluminium and aluminium-silicon carbide composite materials. The results obtained from the experimental studies in the form of break load carrying capacity, peak load carrying capacity, maximum displacement, displacement at break load, stress and stiffness values for the test specimens with different a/d ratios are discussed in the following sections.

A. Peak Load Vs a/d Ratio

The Peak load carrying capacity of the different specimens with different a/d Ratio has been plotted., separately for both isotropic aluminium and Al-SiC composite crack specimen, as shown in Fig. 4. The plot shows a decreasing trend of peak load carrying capacity with increase in initial crack length.

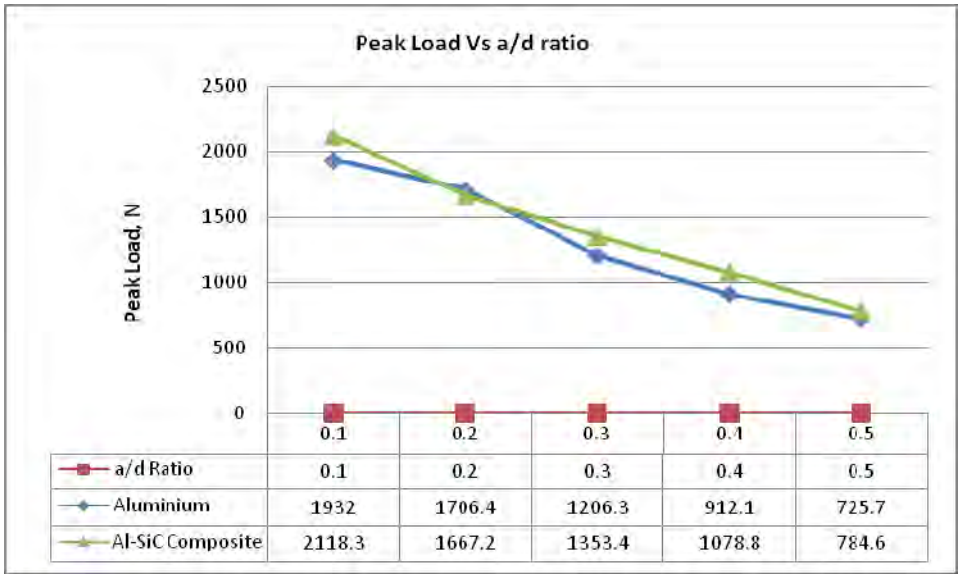

Fig. 4. Peak Load Vs a/d Ratio for both Aluminium and Al-SiC composite Specimens

A close observation reveals that the Al-SiC composite specimen exhibit high peak load carrying capacity than the counterpart isotropic Aluminium specimen for the same initial crack lengths.

B. Break Load Vs a/d Ratio

The break load carrying capacity of the different specimens with different a/d ratio has been plotted, separately for both isotropic Aluminium and Al-SiC composite crack specimen as shown in Fig. 5. The plot shows a decreasing trend of load carrying capacity at the Breaking with increase initial crack length.

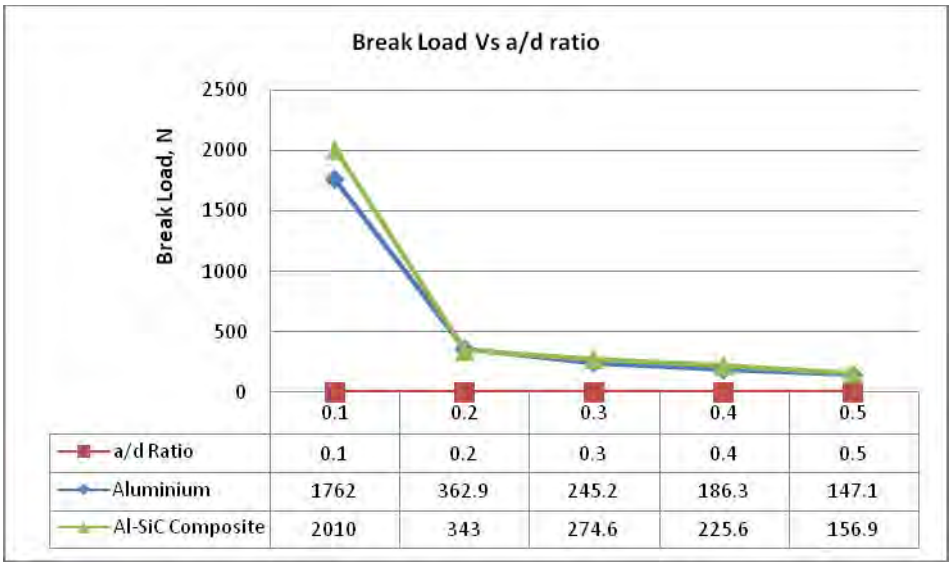

a/d Ratio	0.1	0.2	0.3	0.4	0.5
Aluminium	1762	362.9	245.2	186.3	147.1
Al-SiC Composite	2010	343	274.6	225.6	156.9

Fig. 5. Break Load Vs a/d Ratio for both Aluminium and Al-SiC composite Specimens

A close observation revels that there is a steep drop in the break load carrying capacity from the specimen with a/d ratio 0.1 to a/d ratio 0.2 and there on the plot show a very slight decreasing curve for a/d ratio from 0.2 to a/d ratio 0.5. The plot also reveals that break load for aluminium and Al-SiC composite are very close to each other.

C. Peak Displacement Vs a/d Ratio

The Maximum displacement of different specimens with different a/d Ratio has been plotted, separately for both isotropic Aluminium and Al-SiC composite crack specimen and is shown in Fig. 6. The peak load carried by the aluminium specimens with respective a/d ratio is shown in the brackets.

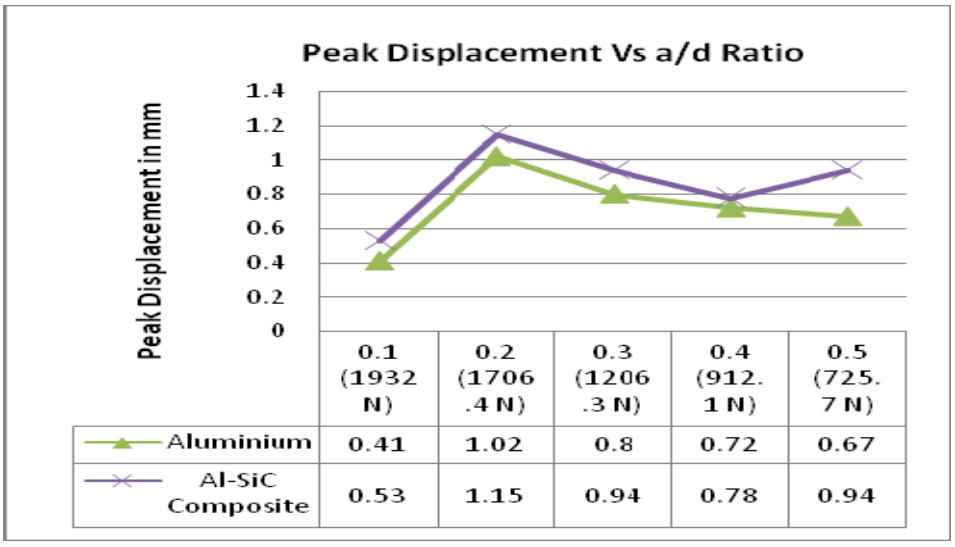

	0.1 (1932 N)	0.2 (1706 .4 N)	0.3 (1206 .3 N)	0.4 (912. 1 N)	0.5 (725. 7 N)
Aluminium	0.41	1.02	0.8	0.72	0.67
Al-SiC Composite	0.53	1.15	0.94	0.78	0.94

Fig. 6. Peak Displacement Vs a/d Ratio for both Aluminium and Al-SiC composite Specimens

The plot reveals that the maximum displacement doesn't follow a regular trend for increasing initial crack length. The plot depicts steep rise in maximum displacement from a/d ratio 0.1 to a/d ratio 0.2 then on it gradually decreases for a/d ratio 0.2 to 0.5.

D. Break Displacement Vs a/d Ratio

The Displacement at breaking of different specimen with different a/d Ratio has been plotted, separately for both isotropic Aluminium and Al-SiC composite Crack specimen. The plot is shown in Fig. 7. The peak load carried by the aluminium-silicon carbide composite specimens with respective a/d ratio is shown in the brackets.

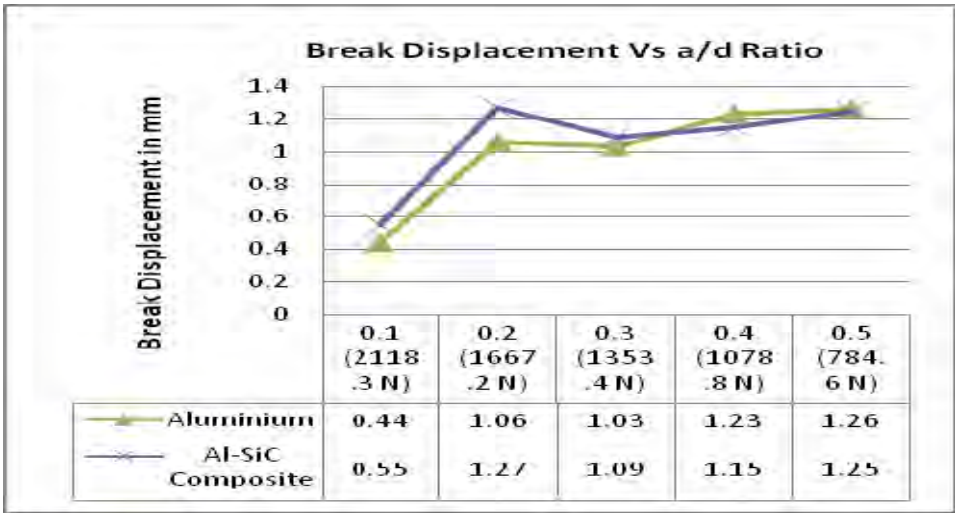

Fig. 7. Break Displacement Vs a/d Ratio for both Aluminium and Al-SiC composite Specimens

The plot depicts a general increasing trend. Under close observation the plot reveals a steep rise in displacement at breaking from a/d ratio 0.1 to 0.2 and there on a gradual increasing trend from a/d ratio 0.2 to a/d ratio 0.5. This trend in case of \ the break displacement coincides with the steep fall in break load from a/d ratio 0.1 to 0.2 and there on a gradual decreasing trend from a/d ratio 0.2 to a/d ratio 0.5.

E. Proof Stress Vs a/d Ratio

The plot depicts Proof Stress of different specimen with different a/d Ratio has been plotted, separately for both isotropic Aluminium and Al-SiC composite Crack specimen. The plot is shown in Fig. 8. The peak load carried by the aluminium specimens with respective a/d ratio is shown in the brackets.

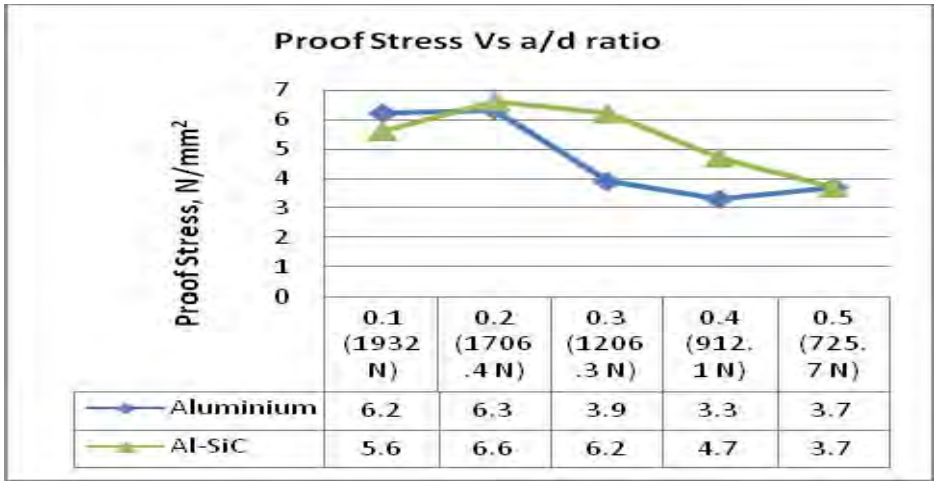

Fig. 8. Proof Stress Vs a/d Ratio for both Aluminium and Al-SiC composite Specimens

The plot depicts a gradual decreasing trend. The plot revels that the stress withstanding capacity of Al-SiC composite Crack specimen is better than its counterpart isotropic Aluminium. Under close observation the plot revels that at a/d ratio 0.5 the stress withstanding capacity of both isotropic Aluminium and Al-SiC composite Crack specimen is almost same. It is inferred that as the initial crack length is made to half of the thickness of the specimens, better stress withstanding capacity of Al-SiC composite over the aluminium gets lost, and both the materials behave alike.

F. Stiffness Vs a/d Ratio

Stiffness of different specimen with different a/d Ratio has been plotted, separately for both isotropic Aluminium and Al-SiC composite Crack specimen. The plot shown in Fig. 9. The peak load carried by the aluminium-silicon carbide composite specimens with respective a/d ratio is shown in the brackets.

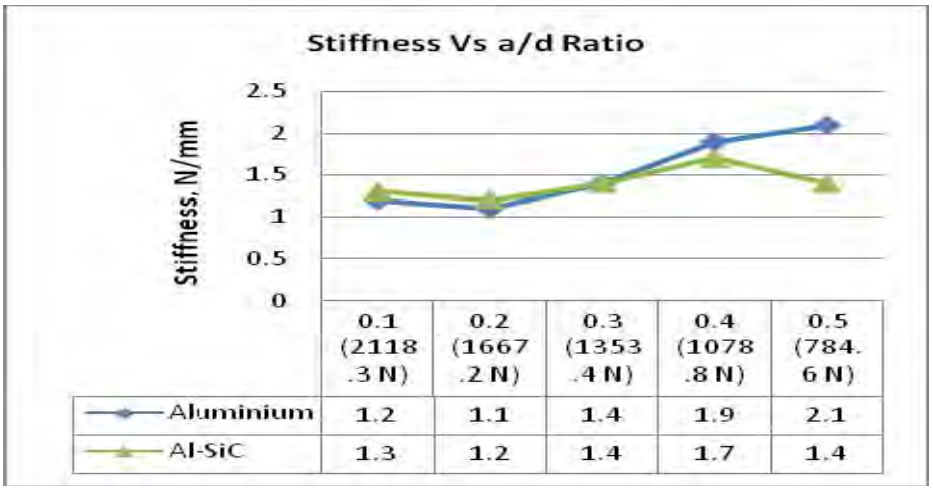

Fig. 9. Stiffness Vs a/d Ratio for both Aluminium and Al-SiC composite Specimens

The plot does not depict a particular trend. This is because the stiffness of the specimen is influenced by many parameters like the length of the specimen, the depth, and also in case of the pre-cracked specimens, the initial crack length is a factor.

G. Ultimate Tensile Strength Vs a/d Ratio

The ultimate tensile strength of different specimens with different a/d Ratio has been plotted, separately for both isotropic Aluminium and Al-SiC composite crack specimen and is shown in Fig. 10 and Fig. 11.

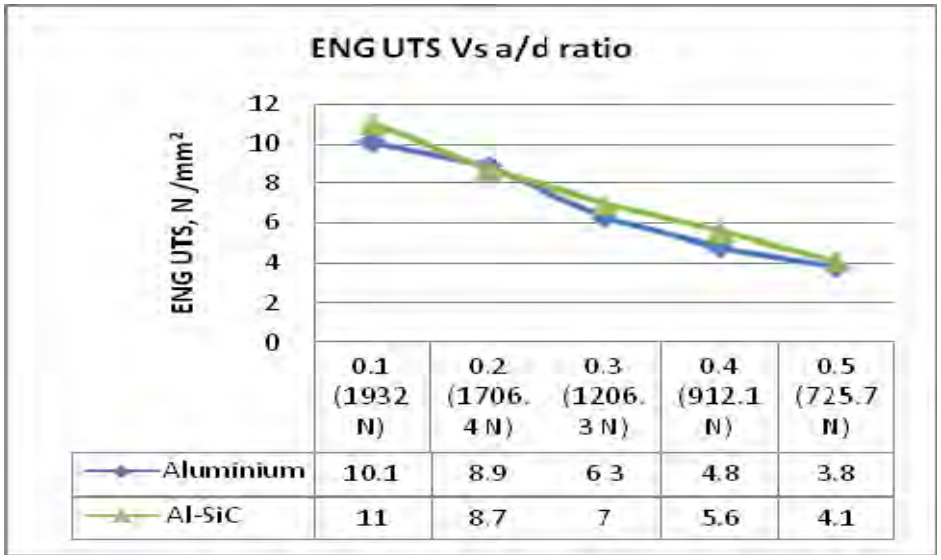

Fig. 10. Engineering UTS Vs a/d Ratio for both Aluminium and Al-SiC composite Specimens

Figure 10 shows the plot of engineering ultimate tensile strength (ENG UTS) of different specimens with different a/d ratios and Fig. 11 shows the plot of true ultimate tensile strength (TRUE UTS) of different specimens with different a/d ratios. The peak load carried by the aluminium specimens with respective a/d ratio is shown in the brackets in Fig. 10 and the peak load carried by the aluminium-silicon carbide composite specimens with respective a/d ratio is shown in the brackets in Fig. 11.

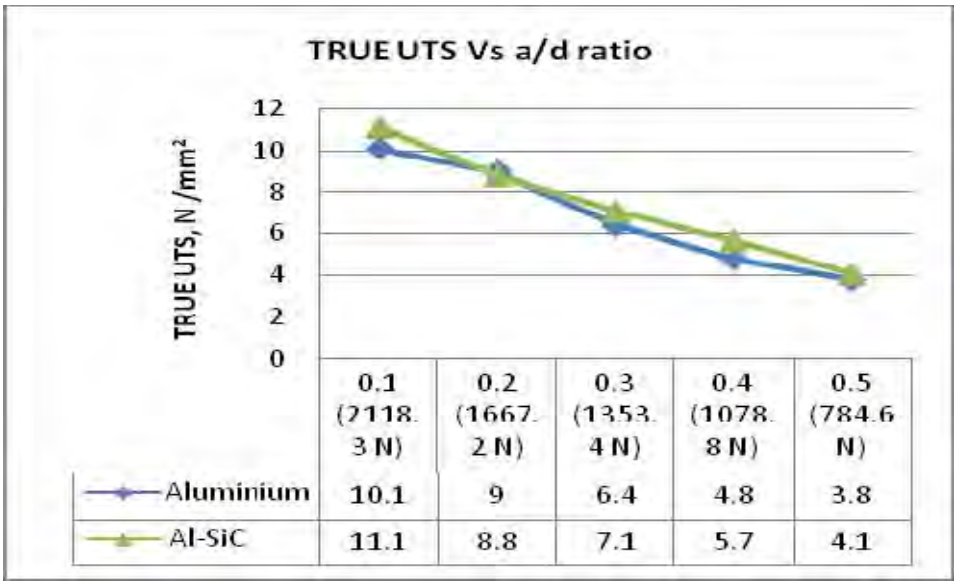

Fig. 11. True UTS Vs a/d Ratio for both Aluminium and Al-SiC composite Specimens

The ultimate tensile strength shows a clear cut decreasing trend with the increasing a/d ratios for both isotropic Aluminium and Al-SiC composite Crack specimens. The interesting point to note here is that the decreasing trend in case of both the materials is almost linear. Moreover, in case of both the engineering ultimate tensile strength (ENG UTS) and true ultimate tensile strength (TRUE UTS) the Al-SiC composite Crack specimens score a slightly higher strength than the Aluminium specimens almost for all different a/d ratios.

IV. Microscopic Studies

The macrostructures and the microstructures obtained using metallurgical microscopes are discussed here. The macrostructures include the fracture location and the fracture propagation. The experimental crack propagation paths are observed under the microscope for different material specimens with different a/d ratios.

A. Macrostructural Study of Aluminium Specimens

The macrostructures obtained using metallurgical microscopes are shown in Fig. 12 to Fig. 15 for aluminium pre-cracked specimens with a/d ratios of 0.2, 0.3, 0.4 and 0.5.

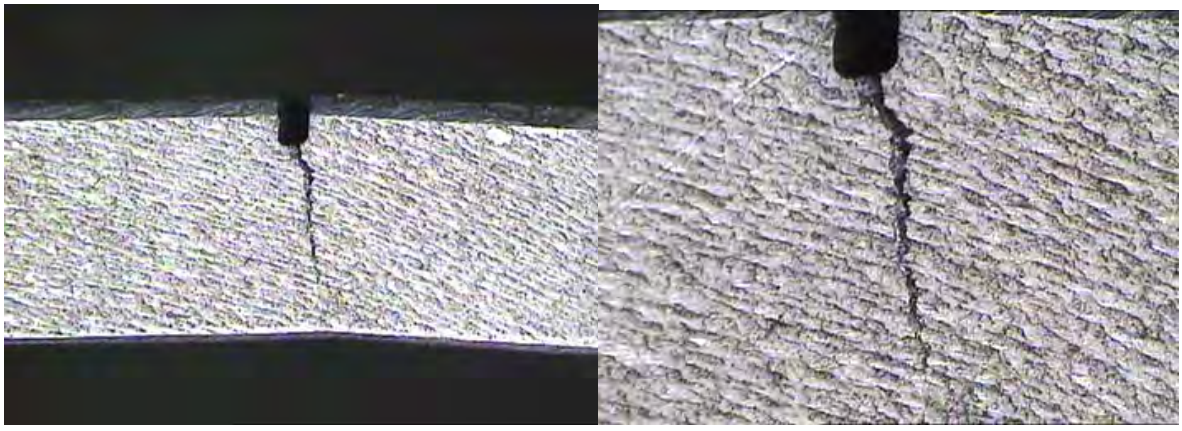

Fig. 12. Crack Growth Path in the Aluminium Specimen with a/d Ratio of 0.2 under 10 X Magnification and 20 X Magnification

Figure 12 shows the Crack Growth Path in the Aluminium Specimen with a/d Ratio of 0.2 under 10 X Magnification and 20 X Magnification. A longer crack growth path is observed in specimens having less a/d ratio compared with the specimens having high a/d ratios.

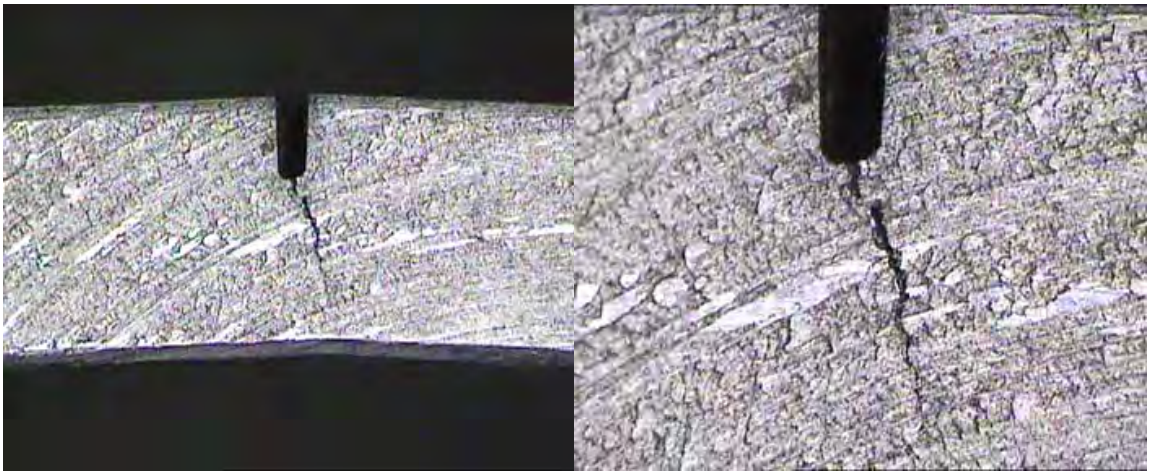

Fig. 13. Crack Growth Path in the Aluminium Specimen with a/d Ratio of 0.3 under 10 X Magnification and 20 X Magnification

Figure 13 shows the Crack Growth Path in the Aluminium Specimen with a/d Ratio of 0.3 under 10 X Magnification and 20 X Magnification.

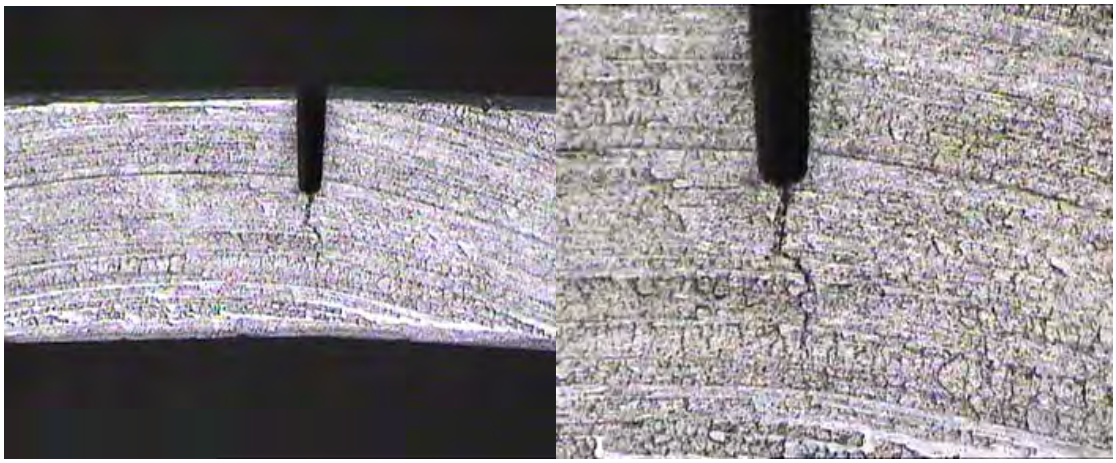

Fig. 14. Crack Growth Path in the Aluminium Specimen with a/d Ratio of 0.4 under 10 X Magnification and 20 X Magnification

Figure 14 shows the Crack Growth Path in the Aluminium Specimen with a/d Ratio of 0.4 under 10 X Magnification and 20 X Magnification.

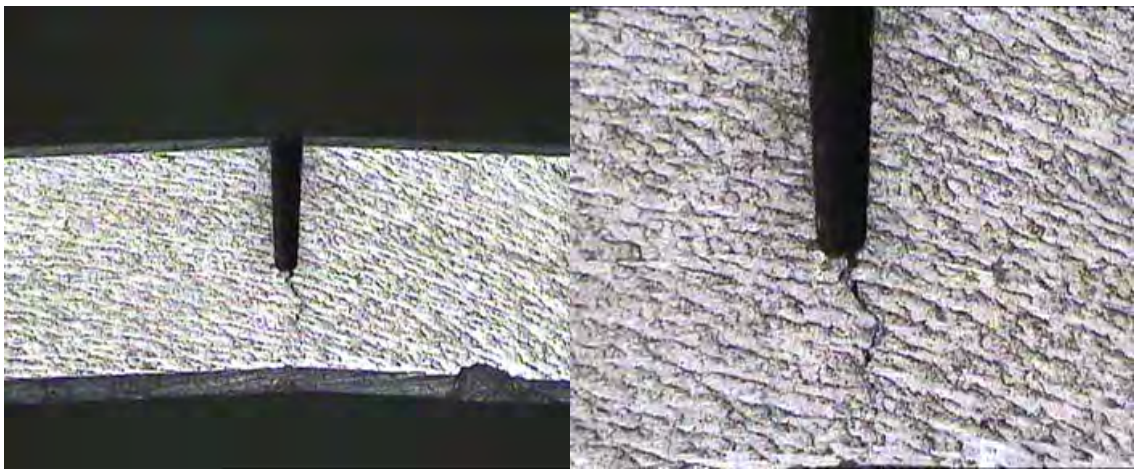

Fig. 15. Crack Growth Path in the Aluminium Specimen with a/d Ratio of 0.5 under 10 X Magnification and 20 X Magnification

Figure 15 shows the Crack Growth Path in the Aluminium Specimen with a/d Ratio of 0.5 under 10 X Magnification and 20 X Magnification. As the initial crack length increases the crack growth path is shortened.

This is because the specimen with higher initial crack lengths could take only lesser load and so the crack grows for a shorter length before it reaches the fracture point.

B. Macrostructural Study of Aluminium-Silicon Carbide Specimens

The macrostructures obtained using metallurgical microscopes are shown in Fig. 16 to Fig. 18 for aluminium-silicon carbide pre-cracked specimens with a/d ratios of 0.2, 0.3 and 0.5.

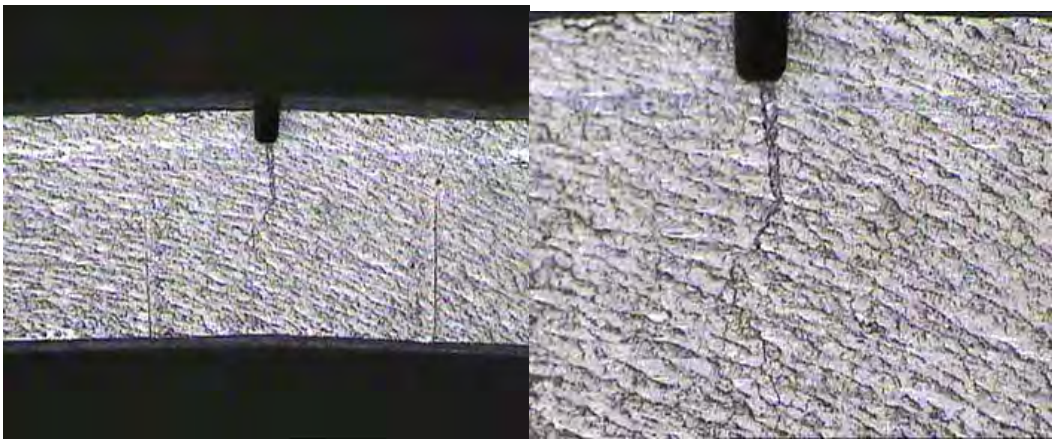

Fig. 16. Crack Growth Path in the Aluminium-Silicon Carbide Specimen with a/d Ratio of 0.2 under 10 X Magnification and 20 X Magnification

Figure 16 shows the Crack Growth Path in the Aluminium-Silicon Carbide Specimen with a/d Ratio of 0.2 under 10 X Magnification and 20 X Magnification.

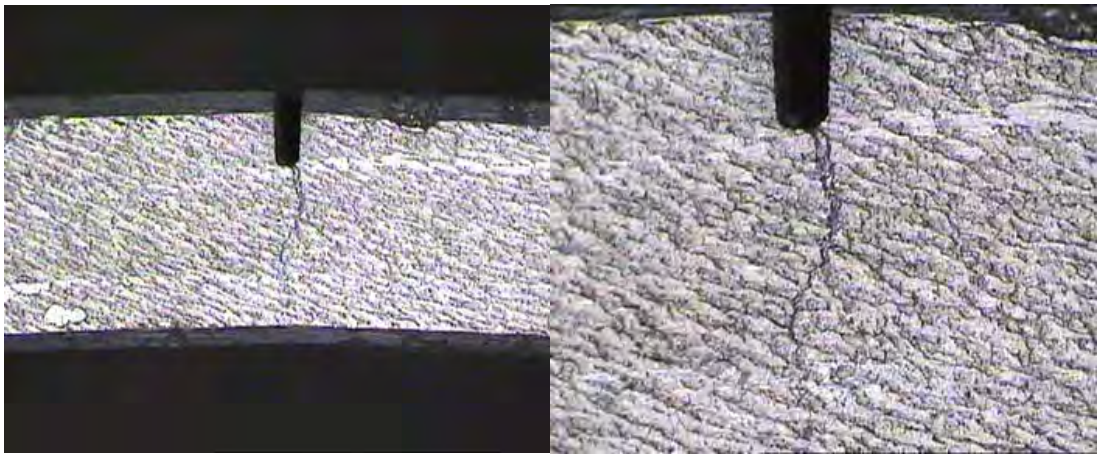

Fig. 17. Crack Growth Path in the Aluminium-Silicon Carbide Specimen with a/d Ratio of 0.3 under 10 X Magnification and 20 X Magnification

Figure 17 shows the Crack Growth Path in the Aluminium-Silicon Carbide Specimen with a/d Ratio of 0.3 under 10 X Magnification and 20 X Magnification.

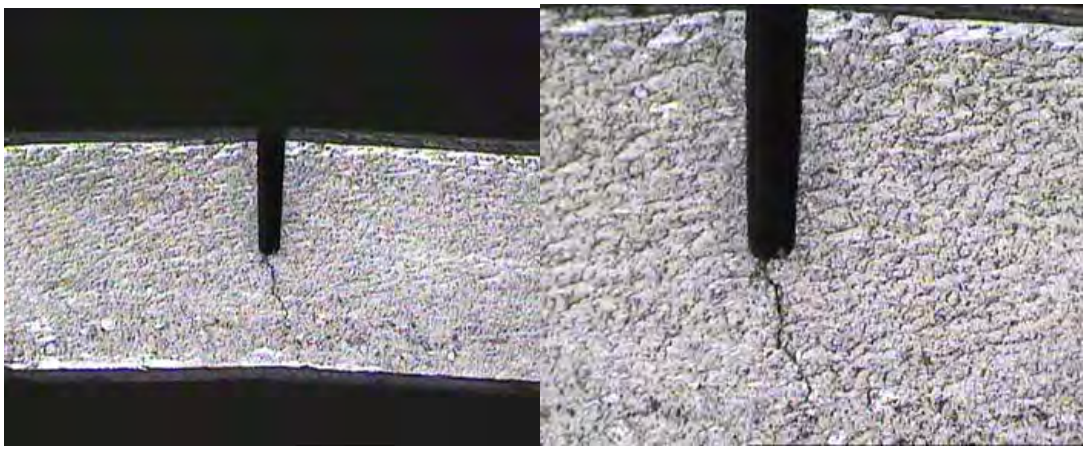

Fig. 18. Crack Growth Path in the Aluminium-Silicon Carbide Specimen with a/d Ratio of 0.5 under 10 X Magnification and 20 X Magnification

Figure 18 shows the Crack Growth Path in the Aluminium-Silicon Carbide Specimen with a/d Ratio of 0.5 under 10 X Magnification and 20 X Magnification.

C. Specimen Preparation for Micro Structural Studies

One set of specimens from both isotropic Aluminium and Al-SiC composite crack specimens were prepared for micro structural studies. The specimens were initially cut to the required size so as to keep under the microscope. The surface to be studied is initially ground to produce a rough even surface using the Belt Grinding machine. Then the surface is polished using a polishing machine with emery sheets of grain size ranging from 120, 240, 320, 400, 600, 800 and 1200. Then finally a smooth polished surface is obtained by using thin cloth polishing.

The etchant used for etching the specimens is called the Keller's Etchant which is an excellent one for Aluminium and Titanium alloys. The composition of the Keller's Etchant is in a 200 ml mixture, distilled water is 190 ml, Nitric acid is 5 ml, Hydrochloric acid is 3 ml and Hydrofluoric acid is 2 ml. The surface is allowed for an immersion of the etchant for about 10-30 seconds. Precaution is to be taken to use only freshly prepared etchants.

D. Micro structural study of Aluminium Specimen

Figure 19 shows the micro structure of the Aluminium Specimen under 50 X Magnification and 100 X Magnification.

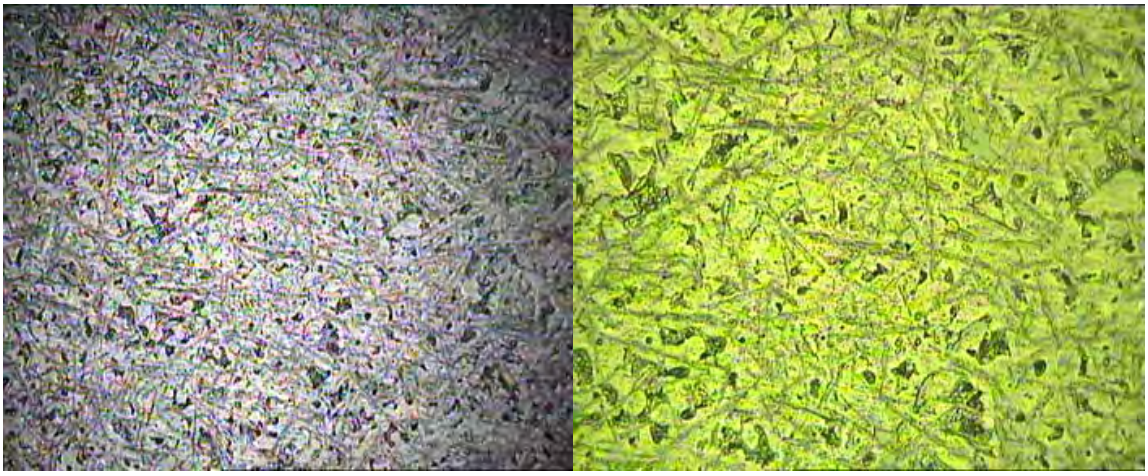

Fig. 19. Microstructure of Aluminium Specimen under 50 X Magnification and 100 X Magnification

Figure 20 shows the micro structure of the Aluminium Specimen under 200 X Magnification and 500 X Magnification.

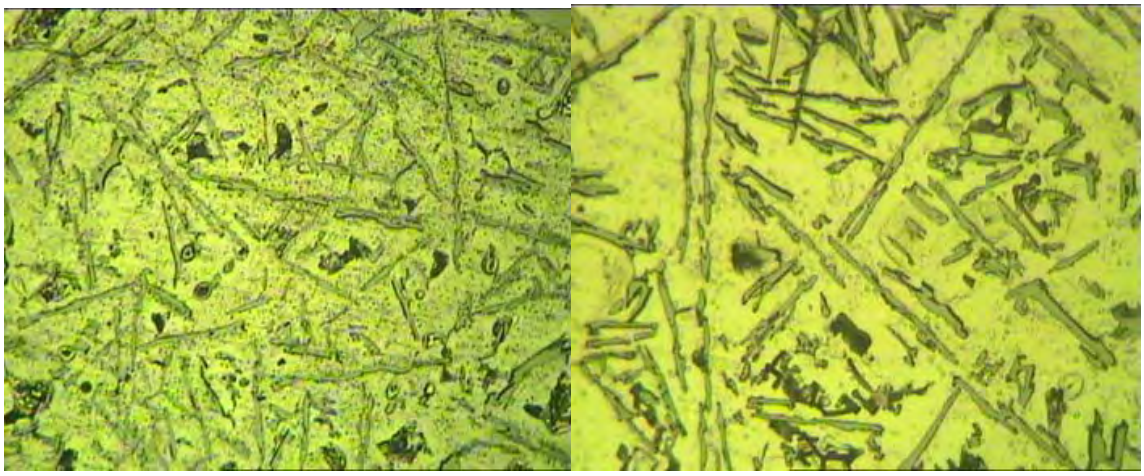

Fig. 20. Microstructure of Aluminium Specimen under 200 X Magnification and 500 X Magnification

Figure 21 shows the micro structure of the Aluminium Specimen under 500 X Magnification in another location.

Fig. 21. Microstructure of Aluminium Specimen under 500 X Magnification at another location

The eutectic particles formed during the casting process are visible in all magnifications. As the aluminium specimens were initially cast the material has shown more tendencies towards brittleness, even though aluminium in general is a ductile material.

E. Micro structural study of Aluminium-Silicon Carbide Specimen

Figure 22 shows the micro structure of the Aluminium-Silicon Carbide Specimen under 50 X Magnification and 100 X Magnification.

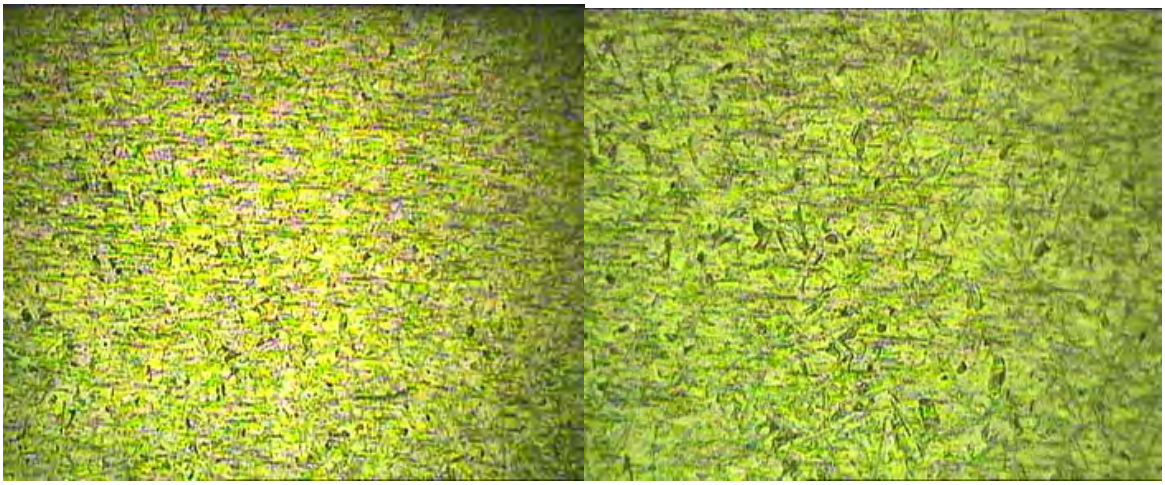

Fig. 22. Microstructure of Aluminium-Silicon Carbide Specimen under 50 X Magnification and 100 X Magnification

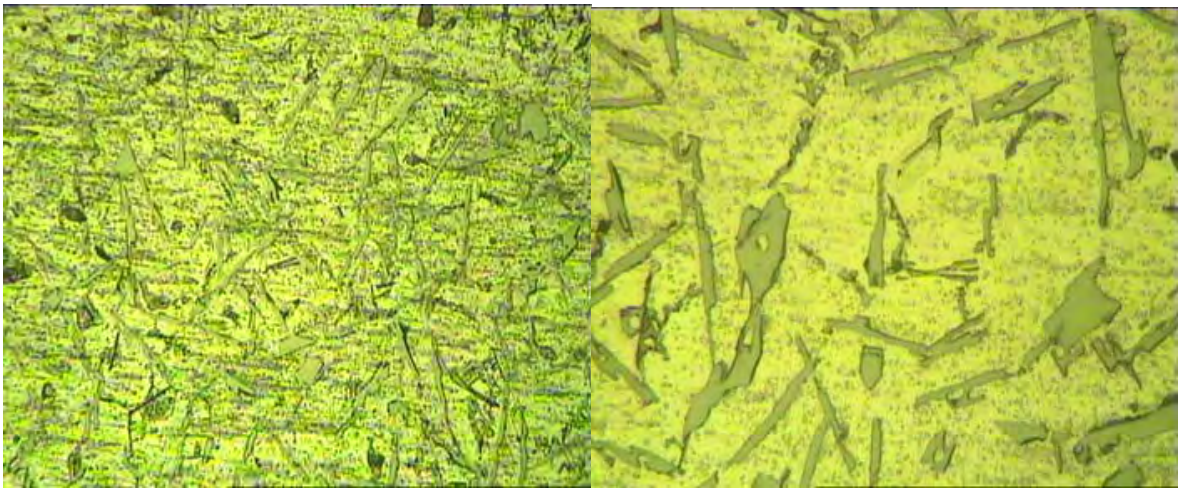

Fig. 23. Microstructure of Aluminium-Silicon Carbide Specimen under 200 X Magnification and 500 X Magnification

Figure 23 shows the micro structure of the Aluminium-Silicon Carbide Specimen under 200 X Magnification and 500 X Magnification.

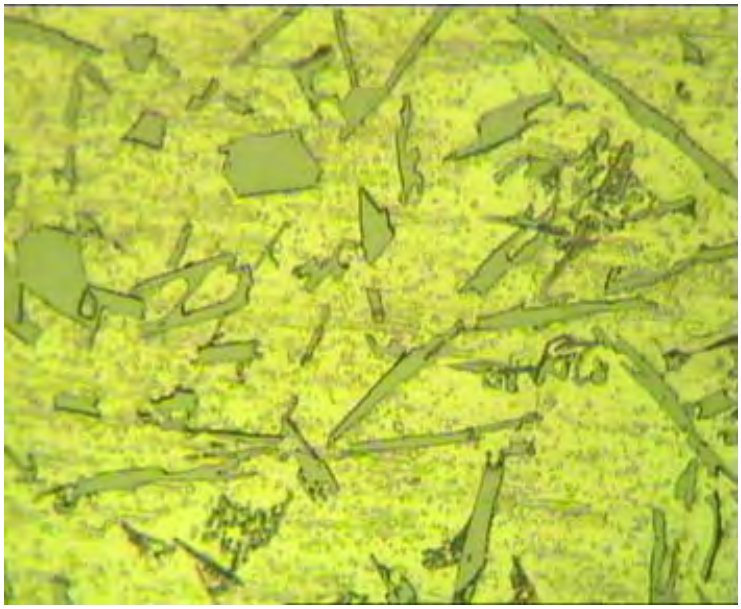

Fig. 24. Microstructure of Aluminium-Silicon Carbide Specimen under 500 X Magnification at another location

Figure 24 shows the micro structure of the Aluminium-Silicon Carbide Specimen under 500 X Magnification at a different location. The presence of the Silicon Carbon in the form of dendrites is visible under all the magnifications. The almost even distribution of silicon carbide is observed indicating the success of the stir casting technique used to produce the aluminium-silicon carbide composite.

V. Conclusion

The fatigue characteristics of both the aluminium and aluminium-silicon carbide composite has been obtained with specimens of different crack length and their ability to survive with the crack is studied. In general, the Al-SiC composite specimens have better fatigue strength than isotropic aluminium specimens for the same a/d ratios. From experimental studies it is observed that aluminium-silicon carbide composite has better Load carrying capacity, proof stress and stiffness which proves that aluminium-silicon carbide is tougher than isotropic aluminium under flexural loading conditions. This proves that aluminium-silicon carbide composites with light weight and low cost are better alternative for aluminium in aerospace structures. The increase in initial crack length decreases the load carrying capacity of the material which has been observed in case of both the aluminium and aluminium-silicon carbide composite. It has also been observed that irrespective of the material, for a crack length with a/d ratio of 0.5 and more has similar effects. The studies have revealed that Al-SiC Composite has slightly better advantage over isotropic aluminium in terms of fatigue life.

The macrostructural studies have been done on both aluminium and Al-SiC composite specimens with the different a/d ratios to observe the experimental crack growth path and have been reproduced. The crack grows for longer length for specimens with less initial crack lengths. As the initial crack length increases the crack growth path is shortened. This is because the specimen with higher initial crack lengths could take only lesser load and so the crack grows for a shorter length before it reaches the fracture point. This crack growth path could be compared against the crack growth paths obtained using simulation techniques. The micro structural studies on the aluminium and Al-SiC composite specimens have been done under different magnifications. The presence of eutectic particles formed during the cooling process in case of aluminium cast specimens has been observed. The presence of the silicon-carbide dendrites embedded into the aluminium matrix dislocations has been observed. The silicon-carbide dendrites been observed to be almost evenly distributed. The aluminium matrix contains high amount of dislocations, responsible for the strength of the Al-SiC composite material. The dislocations are introduced during cooling by the SiC particles, due to their different thermal expansion coefficient.

Acknowledgment

The authors wish to acknowledge Tagore Engineering College, Chennai, Tamilnadu, India, and the Department of Mechanical Engineering for having permitted to use their facilities to conduct the three point bend test and the microscopic studies.

REFERENCES

[1] D. L. Mcdanels, "Analysis of stress-strain, fracture, and ductility behavior of aluminium matrix composites containing discontinuous silicon carbide reinforcement," J Metal. Trans. A, vol. 16A, pp. 1104-1105, 1985.

[2] M. G. Kulakarni, S. Pal, and D. V. Kubair, "Mode-3 spontaneous crack propagation in unsymmetric functionally graded materials," Int. J Solids Struct., vol. 44, pp. 229-241, 2007.

[3] L. Marin, "Numerical solution of the Cauchy problem for steady-state heat transfer in two-dimensional functionally graded materials," Int. J Solids Struct., vol. 42, pp. 4338-4351, 2005.

[4] N. Cherradi, A. Kawasaki, and M. Gasik, "Worldwide trends in functional gradient materials research and development," Compos. Engg., vol. 8, pp. 883-894, 1994.

[5] A. J. Markworth, K. S. Ramesh, and W. P. Parks Jr., "Review: Modelling studies applied to functionally graded materials," J Mater. Sci., vol. 30, pp. 2183-2193, 1995.

[6] T. Hirano, and K. Wakashima, "Mathematical modelling and design of FGMs," Mrs. Bull., vol. 20(1), pp. 40-42, 1995.

[7] A. Neubrand, and J. Rodel, "Gradient materials: An overview of a novel concept," Zeit. F. Met., vol. 88, pp. 358-371, 1997.

[8] A. Mortensen, and S. Suresh, "Functionally graded metals and metal-ceramic composites: Part 1 Processing," Int. Mater. Rev., vol. 30, pp. 2183-2193, 1995.

[9] F. Erdogan, "Fracture mechanics of functionally graded materials," Mater. Res. Soc. Bull., vol. 20(1), pp. 43-44, 1995.

[10] F. Erdogan, "Fracture mechanics of functionally graded materials," Compos. Eng., vol. 5(7), pp. 753-770, 1995.

[11] M. T. Tilbrook, R. J. Moon, and M. Hoffman, "Crack propagation in graded composites," Compo. Sci. Tech., vol. 65, pp. 201-220, 2005.

[12] M. T. Tilbrook, R. J. Moon, and M. Hoffman, "Finite element simulations of crack propagation in functionally graded material under flexural loading," Engng. Frac. Mech., vol. 72, pp. 2444-2467, 2005.

[13] C. Li, Z. Zou, and Z. Duan, "Stress intensity factors for functionally graded solid cylinders," Engng. Frac. Mech., vol. 63, pp. 735-749, 1999.

[14] Z. J. Zhang, and G. H. Paulino, "Cohesive zone modeling of dynamic failure in homogeneous and functionally graded materials," Int. J Plast., Vol. 21, pp. 1195-1254, 2005.

[15] J. H. Kim, and G. H. Paulino, "Mixed-mode fracture of orthotropic functionally graded materials using finite elements and the modified crack closure method," Engng. Frac. Mech. Vol. 69, pp. 1557-1586, 2002.

[16] C. Comi, and S. Mariani, "Extended finite element simulation of quasi-brittle fracture in functionally graded materials," Com. Methods Appl. Mech. Engng., vol. 196, pp. 4013-4026, 2007.

[17] M. T. Tilbrook, K. Rozenburg, E. D. Steffler, L. Rutgers, and M. Hoffman, "Crack propagation paths in layered, graded composites," Comp. Engng., vol. 37, pp. 490-498, 2006.

[18] D. J. Shim, G. H. Paulino, and R. H. Dodds Jr., "Effect of material gradation on K-dominance of fracture specimens," Engng. Frac. Mech., vol. 73, pp. 643-648, 2006.

[19] Z. H. Jin, G. H. Paulino, and R. H. Dodds Jr., "Cohesive fracture modeling of elastic-plastic crack growth in functionally graded materials," Engng. Frac. Mech., vol. 70, pp. 1885-1912, 2003.

[20] M. C. Walters, G. H. Paulino, and R. H. Dodds Jr., "Stress-intensity factors for surface cracks in functionally graded materials under mode-I thermomechanical loading," Int. J Solids Struct., vol. 41, pp. 1081-1118, 2004.

[21] A. M. Afsar, Anisuzzaman, and J. I. Song, "Inverse problem of material distribution for desired fracture characteristics in a thick–walled functionally graded material cylinder with two diametrically-opposed edge cracks.," Engng. Frac. Mech. Vol. 76, pp. 845-855, 2009.

[22] A. M. Afsar, and Anisuzzaman, "Stress intensity factors of two diametrically opposed edge cracks in a thick-walled functionally graded material cylinder," Engng. Frac. Mech. Vol. 74, pp. 1617-1636, 2007.

[23] P. Hvizdos, D. Jonsson, M. Anglada, G. Anne, and O. V. D. BIest, "Mechanical properties and thermal shock behaviour of an alumina/zirconia functionally graded material prepared by electrophoretic deposition," J Eur. Ceram. Soc. Vol. 27, pp. 1365-1371, 2007.

[24] Q. G. Wang, "Microstructural effects on the tensile and fracture behavior of aluminium casting alloys A356/357," Met. Mater. Trans A., vol. 34A, pp. 287-2899, December 2003.

[25] C. Neelima Devi, N. Selvaraj, and V. Mahesh, "Micro structural aspects of aluminium silicon carbide metal matrix composite," Int. J App. Sci. Engg. Res. Vol. 1, No. 2, pp. 250-254, 2012.

[26] Z. Li, W. Yuan-jie, Y. Xian-wang, C. Shu, and X. Xiang-jun, "Crack propagation characteristic and toughness of functionally graded WC-Co cemented carbide.," Int. J Refract. Metals. Hard Mater., vol. xxx, pp. xxx_xxx, 2007.

[27] H. G. Lambers, B. Gorny, Tschumak, H. J. Maier, and D. Canadinc, "Crack growth behavior of low-alloy bainitic 51CrV4 steel," Procedia Engng., vol. 2, pp. 1373-1382, 2010.

[28] S. J. Lee, J. Wang, and B. V. Sankar, "A micromechanical model for predicting the fracture toughness of functionally graded foam," Int. J Solids Struct. Vol. 44, pp. 4053-4067, 2007.

[29] V. Camillo, T. Manfredini, M. Montorsi, C. Siligardi, and A. Sola, "Microstructure-based modeling and experimental investigation of crack propagation in glass-alumina functionally graded material," J Esssur. Ceram. Soc. Vol. 26, pp. 3067-3073, 2006.